Study of Poly(methyl methacrylate) Stereocomplex Formation by Nonradiative Energy Transfer and by Time-Resolved Fluorescence Spectroscopy

Drahomír Vyprachtický,* Veronika Pokorná, Jan Pecka, and František Mikeš

Institute of Macromolecular Chemistry, Academy of Sciences of the Czech Republic, Heyrovský Sq. 2, 162 06 Prague 6, Czech Republic

Received June 25, 1997; Revised Manuscript Received September 26, 1997[⊗]

ABSTRACT: Poly(methyl methacrylate)s labeled with a fluorophore donor, carbazole (C), or acceptor, anthracene (A), have been prepared by free radical, anionic, and coordination polymerization, yielding atactic (a), isotactic (i), and syndiotactic (s) polymers. Nonradiative energy transfer (NET) was used to study polymer association in solutions. The efficiency of NET for mixtures of labeled tactic poly(methyl methacrylate)s ($C_{POL} = 5.00$ g L^{-1}; $C_C = 2.61 \times 10^{-4}$ M; $C_A = 6.00 \times 10^{-4}$ M) in dimethylformamide and dioxane was 0.20 and 0.10, respectively. For a mixture of atactic polymers, the efficiency of NET in the same solvents under similar conditions is much lower. The efficiency of NET for a mixture of labeled atactic poly(methyl methacrylate)s increases with increasing polymer concentration and is nearly independent of concentration for a mixture of labeled tactic polymers. The time-dependent decays of fluorescence anisotropy show that stereocomplexation causes an increase in rotational correlation times of carbazole and anthracene fluorophores. The rotational correlation time of carbazole fluorophore as a part of a stereocomplex is 25.5 and 19.1 ns in dimethylformamide and dioxane, respectively, and shorter than 2 ns in noncomplexing solvents.

Introduction

Syndiotactic and isotactic poly(methyl methacrylate)s (s-PMMA and i-PMMA) form a stereocomplex in some solvents. The formation and structure of this stereocomplex have been studied by a variety of methods,[1] i.e., turbidity, light scattering, sedimentation, osmometry, GPC, viscometry, DSC, X-ray diffraction, NMR, IR spectroscopy, and nonradiative energy transfer (NET).[2]

In NET, the electronic excitation energy is transferred from a donor to an acceptor fluorophore through an induced resonance interaction if the emission spectrum of the donor overlaps the absorption spectrum of the acceptor. The theory for this resonance nonradiative energy transfer was derived by Förster[3−5] using a dipole−dipole approximation of Coulombic interactions. The rate of the transfer was predicted to be inversely proportional to the sixth power of the distance between the interacting fluorophores and thus very sensitive to this distance. NET has been used extensively to characterize intramolecular distances in biological macromolecules.[6] A number of studies have also been reported, dealing with intermolecular and intramolecular NET in synthetic polymers. NET has been used for the characterization of polymer compatibility,[7−9] in the study of conformational properties of macromolecules in solution and their dynamics,[10−13] in the study of molecular association in polymer solutions[2,14,15] and many other applications.[16,17] Reviews are available summarizing polymer studies to 1988 and up to 1993 employing NET.[18,19]

In a preliminary study[2] it was shown that stereocomplex formation between carbazole (C) and anthracene (A) labeled PMMA is accompanied by a decrease in the ratio of carbazole and anthracene emission intensities I_C/I_A. The dependence of I_C/I_A on the content of s-PMMA in the mixture confirmed the relative tendency for stereocomplex formation in various solvents and revealed its stoichiometry (e.g., i-PMMA/s-PMMA = 1:2 in DMF).

By comparison with a previous study, time-resolved fluorescence measurements of the carbazole fluorophore in the absence and presence of the anthracene fluorophore allow us to evaluate quantitatively the efficiency of NET in systems where stereocomplex formation does or does not take place. Such a comparison has unambiguously proved the stereocomplex formation.

From time-resolved fluorescence anisotropy studies the rotational correlation times of donor and acceptor fluorophores in the stereocomplex have been determined. These rotational correlation times were compared with the correlation times for fluorophores imbedded in noncomplexing polymers.

Experimental Section

Monomers. 2-(9-Carbazoyl)ethyl methacrylate (CEMA) was prepared by a reaction of methacryloyl chloride with 9-(2-hydroxyethyl)carbazole in toluene according to the procedure used for the preparation of 3-(*N*-carbazoyl)propyl methacrylate;[20] triethylamine was used as the hydrogen chloride acceptor. The product was crystallized from heptane; mp 82−83.5 °C. Anal. Calc: C, 77.40; H, 6.13; N, 5.01. Found: C, 77.36; H, 6.16; N, 4.91.

The structure of CEMA was confirmed by IR and NMR spectrometry. The product was homogeneous on TLC. The molar absorption coefficient was $\epsilon_{292} = 16\,800$ L mol^{-1} cm^{-1} (dioxane). *N*-(2-Hydroxyethyl)carbazole was prepared by a reaction of carbazole with ethylene oxide in the presence of potassium hydroxide in methyl ethyl ketone.[21] The product was isolated by pouring the reaction mixture into water. The crude product was dissolved in toluene, and after addition of heptane N-(2-hydroxyethyl)carbazole crystallized.

(9-Anthryl)methyl methacrylate (AMMA) was prepared (analogously as CEMA) by a reaction of methacryloyl chloride with 9-(hydroxymethyl)anthracene. The crude product was crystallized from a binary mixture of toluene/heptane and recrystallized from methanol; mp 82−84 °C (ref.[22] 82−83 °C). Anal. Calc: C, 82.58; H, 5.84. Found: C, 82.76; H, 5.79. The structure of AMMA was confirmed by IR and NMR spectrometry. The product was homogeneous on TLC. The molar absorption coefficients were $\epsilon_{366} = 8460$ L mol^{-1} cm^{-1} and $\epsilon_{292} = 323$ L mol^{-1} cm^{-1} (dioxane).

[⊗] Abstract published in *Advance ACS Abstracts,* November 15, 1997.

S0024-9297(97)00934-0 CCC: $14.00

Table 1. Microstructure, Content of Fluorophores, and Molar Weights of Homopolymers and Copolymers of Methyl Methacrylate

polymer	tacticity (%) I	H	S	label content (mol %)	$10^{-3}M_n$	$10^{-3}M_w$
a-PMMA-C	3.9	32.6	63.5	1.12	51	123
a-PMMA-A	4.6	34.7	60.7	1.09	57	136
a-PMMA	3.9	34.1	62.0	0.00	45	84
i-PMMA-C	71.9	11.1	17.0	1.61	3	7
i-PMMA-A	84.1	3.7	12.2	0.69	6	10
i-PMMA	95.0	3.0	2.0	0.00	16	19
s-PMMA-C	2.2	11.4	86.4	1.75	60	568
s-PMMA-A	3.5	13.8	82.7	1.86	40	433
s-PMMA	0.8	9.0	90.2	0.00	64	278

9-(Hydroxymethyl)anthracene was either a commercial product (Aldrich) or it was prepared by reduction of 9-anthraldehyde with sodium borohydride in methanol.

Homopolymers and Copolymers. Unlabeled Polymers. Atactic poly(methyl methacrylate) (a-PMMA) was prepared by free radical polymerization of methyl methacrylate (MMA) in toluene at 60 °C using AIBN [2,2′-azobis(2-methylpropionitrile)] initiator. The polymer was reprecipitated into methanol. Isotactic PMMA (i-PMMA) was prepared by anionic polymerization of MMA in toluene at −78 °C using *tert*-butylmagnesium bromide initiator.[23] Syndiotactic PMMA (s-PMMA) was prepared by polymerization of MMA initiated by $TiCl_4-Et_3$ Al at −78 °C in toluene.[24]

Labeled Polymers. Fluorescent labels were introduced into PMMA by copolymerization of MMA with CEMA or AMMA. Copolymerizations were carried out in the same way as the preparation of unlabeled polymers. Atactic PMMA was labeled with carbazole (a-PMMA-C) or anthracene (a-PMMA-A), isotactic PMMA with anthracene (i-PMMA-A) or carbazole (i-PMMA-C), and syndiotactic PMMA with carbazole (s-PMMA-C) or anthracene (s-PMMA-A).

Characterization. Molecular weights were determined by GPC using tetrahydrofuran solutions and a Hewlett-Packard 1090 apparatus controlled by a HP 85B computer. PL gel 10 μ MIXED or PL gel 10 μ 500 (Polymer Laboratories Ltd., Shropshire, U.K.) columns were used for analysis. The apparatus was calibrated using atactic PMMA (M_w/M_n < 1.05, Polymer Standard Service, Mainz, FRG) standards. The molecular weight averages were calculated using a program supplied by Hewlett Packard.

UV−vis spectra were taken on a Hewlett-Packard 8451A spectrophotometer.

^{1}H NMR spectra were taken on a Bruker ACF-300 spectrometer at 300.1 MHz in deuterium chloroform at 60 °C using hexamethyldisiloxane as an inner standard.

The content of syndiotactic (S), heterotactic (H), and isotactic (I) triads in the homopolymers and the copolymers of methyl methacrylate with a low content of fluorophore monomers was determined[25] from integrated intensities of the α-CH_3 signals at 0.80 ppm (rr), 1.00 ppm (mr), and 1.15 ppm (mm) in 10 wt % solution of polymers. The content of carbazole and anthracene fluorophores in copolymers was evaluated by UV−vis spectrometry in dioxane solutions. The molar absorption coefficients of CEMA and AMMA were used for calculation (Table 1).

Steady-State Fluorescence Measurements. Fluorescence spectra were measured with a Hitachi Perkin-Elmer MPF-2A spectrometer provided with a Hamamatsu R928 photomultiplier and were corrected for the wavelength dependence of the instrument sensitivity.[26] The spectral sensitivity coefficient was determined using a tungsten bulb having a known spectral distribution and standard fluorescence spectra[27−29] of β-naphthol and *m*-nitrodimethylaniline.

To determine the I_C/I_A ratio, solutions of labeled polymers were diluted with the corresponding unlabeled polymers to attain the desired concentration and i- to s-PMMA ratio. The complexation was studied in dioxane, dimethylformamide, and chloroform. Reflectance fluorescence spectra were measured at 24 °C. The donor was excited at 292 nm, and the energy transfer efficiency was characterized by the ratio of the emission intensity of the donor at 345 nm (I_C) and the acceptor at 411 nm (I_A).

Table 2. Relative Fluorescence Quantum Yield (Q_D) of Carbazole Fluorophore and Values of the Overlap Integral (J) and Characteristic Distance (R_o) for Donor−Acceptor Pair Carbazole−Anthracene (AMMA) in Different Solvents

carbazole fluorophore	solvent	Q_D	R_o (nm)	$10^{15}J$ (L mol^{-1} cm^3)
CEMA	dioxane	0.36	2.73	8.15
a-PMMA-C	dioxane	0.49	2.89	8.11
a-PMMA-C	DMF	0.57	2.97	8.47

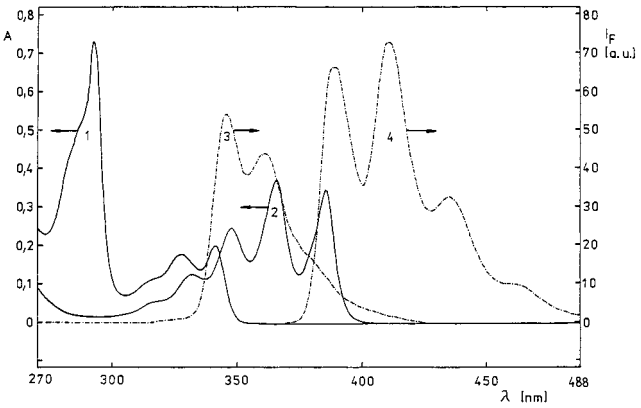

Figure 1. Absorption spectra of CEMA (1) and AMMA (2) at concentration 4.36 × 10^{-5} M and emission spectra of CEMA (3) (ex = 292 nm) and AMMA (4) (ex = 366 nm) at concentrations equal to 0.1 absorbance at the excitation wavelength in dioxane.

Fluorescence Quantum Yield. The relative fluorescence quantum yield (Q_D) of carbazole fluorophore (donor) in the low molecular weight analogue and in copolymers was calculated[30] from

$$Q_D = Q_S \frac{A_S}{A} \frac{n^2}{n_S^2} \frac{\int_\lambda I(\lambda)\, d\lambda}{\int_\lambda I_S(\lambda)\, d\lambda} \quad (1)$$

where subscript S denotes a standard compound, A is the absorbance of a solution at the excitation wavelength, n is the refractive index of the solvent, and $I(\lambda)$ is the intensity of fluorescence at the emission wavelength λ. The "inner filter effect" was eliminated using solutions having the same optical density (A = 0.1) at the wavelength of excitation. The fluorescence quantum yield[31] of carbazole in cyclohexane is Q_S = 0.38. The excitation wavelength was at the maximum of the absorption band (standard, ex = 290 nm and em = 310−420 nm; copolymers, ex = 292 nm and em = 330−440 nm). The area under the emission spectrum was evaluated by numeric integration of corrected emission spectra. The relative quantum yields are given in Table 2. The values of the overlap integral J in Förster's theory for the low molecular weight carbazole monomer and carbazole fluorophore embedded in the polymer chain and the anthracene fluorophore (AMMA) in different solvents are summarized in Table 2.

Figure 1 illustrates absorption and emission spectra of CEMA and AMMA in dioxane.

Characteristic Distance (R_o) and Efficiency of Nonradiative Energy Transfer. The characteristic (Förster) distance (R_o) at which the transfer rate is equal to the decay rate of the donor in the absence of acceptor is given (for fluorophores separated at constant distance, no diffusion during the excited lifetime of donor) by

$$R_o^6 = \frac{9000(\ln 10)K^2 Q_D}{128\pi^5 N_A n^4} \int_0^\infty \frac{I_D(\nu)\, \epsilon_A(\nu)\, d\nu}{\nu^4} = 8.8 \times 10^{-25} \times (K^2 n^{-4} Q_D J)\ (\text{cm}^6) \quad (2)$$

where Q_D is the fluorescence quantum yield of the donor in the absence of acceptor, n is the refractive index of the medium, N_A is Avogadro's number, $I_D(\nu)$ is the corrected fluorescence intensity of the donor in the wave number range ν to $\nu + d\nu$ with the total intensity normalized for unity, $\epsilon_A(\nu)$ is the molar absorption coefficient of the acceptor, and J is the spectral overlap integral between the donor-corrected emission and the acceptor absorption spectrum. The factor K^2 is known to be 2/3 for a random mutual orientation of the transition moments of the donor and acceptor if the rotational correlation time is short compared to their excited-state lifetime (dynamic averaging), while it is 0.476 in rigid media (static averaging).[32] This mutual orientation is certainly random in noncomplexing solutions of donor- and acceptor-labeled polymers, and we may assume it to be random even in a stereocomplex with a low fluorophore content. Whereas the dynamic averaging can be expected to apply for labels attached to isolated chains, this may not be so for labels attached to the rigid stereocomplex. However, eq 2 shows that R_0 is affected very little by a change from dynamic to a static averaging. The efficiency of nonradiative energy transfer (E) was calculated from the average lifetime of the donor (carbazole) fluorescence in the presence (τ_{DA}) and absence (τ_D) of the acceptor

$$E = 1 - \frac{\tau_{DA}}{\tau_D} \tag{3}$$

Time-Resolved Fluorescence Measurements. Time-dependent decays of fluorescence anisotropy and average lifetimes of the excited state were obtained using a time-resolved fluorometer FL 900 CDT (Edinburgh Analytical Instruments, Edinburgh, U.K.). This apparatus uses the time-correlated single photon counting method.

Time-resolved decays of fluorescence intensity were analyzed by deconvolution of the lamp pulse with the impulse response of the sample. The observed decay intensity of fluorescence $R(t)$ is given by the convolution integral[26]

$$R(t) = \int_0^t F(t - t')\, L(t')\, dt' \tag{4}$$

where $L(t)$ is the time distribution of the lamp pulse and $F(t)$ is the response (theoretical) function corresponding to the infinitely short excitation lamp pulse. $L(t)$ was measured using a solution of LUDOX (DuPont) closely spaced in time to particular fluorescence decay experiments (Figure 2).

The time-resolved decay of fluorescence intensity obtained by computer using FL900CDT software is given by

$$F(t) = A + \sum_i B_i \exp(-t/\tau_i) \tag{5}$$

where B_i is a preexponential factor representing the fractional contribution to the time-resolved decay of the component with a lifetime τ_i, A is the background, and t is time.

Least-squares analysis of the time-resolved decay was used for estimation of the impulse response function $F(t)$. The goodness of fit (χ^2) was calculated from

$$\chi^2 = \sum_t \frac{[R(t) - R_C(t)]^2}{R(t)} \tag{6}$$

where $R_C(t)$ is the calculated decay of fluorescence. The fractional intensity of each species is given by

$$\text{rel } B_i = \frac{B_i \tau_i}{\sum_i B_i \tau_i} 100 \tag{7}$$

The time-resolved intensity decays of the parallel [$R_{VV}(t)$] and the perpendicular [$R_{VH}(t)$] components of the emission were measured, and the time-resolved anisotropy $r(t)$ was

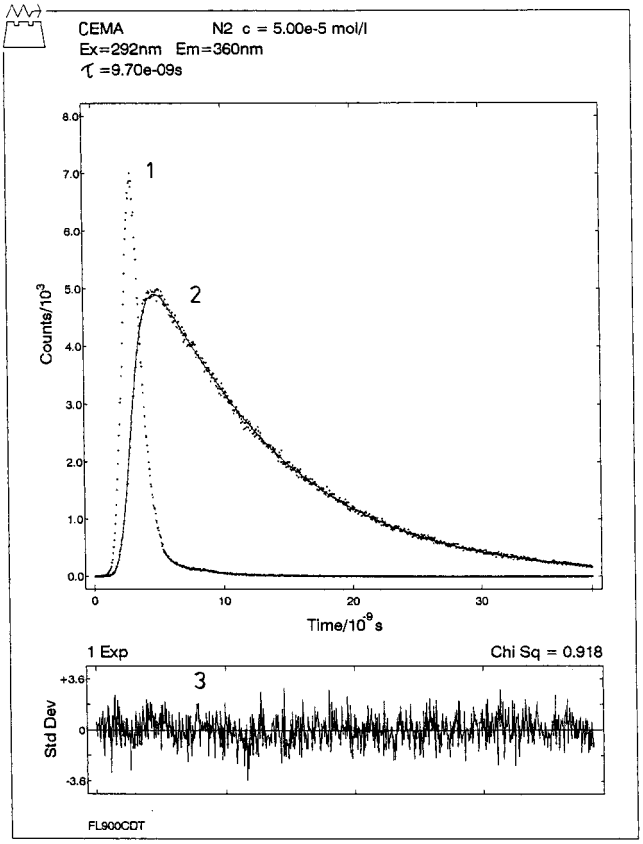

Figure 2. Time-resolved fluorescence decay for CEMA in dioxane: the measured lamp pulse (1), the calculated fluorescence decay $R_c(t)$ from experimental points (2), and the standard deviation (3).

calculated point by point using the equation

$$r(t) = \frac{GR_{VV}(t) - R_{VH}(t)}{GR_{VV}(t) + 2R_{VH}(t)} \tag{8}$$

where $G = \sum_t R_{HH}(t)/\sum_t R_{HV}(t)$.

The emission anisotropy $r(t)$ was analyzed using the experimental function (eq 5) without deconvolution; τ_i is in this case the rotational correlation time (Φ_i) of the fluorophore, and A is a limiting anisotropy (r_∞).

Excitation of the samples was carried out by a pulse lamp nF 900 controlled by a thyratron tube having a repetition frequency rate 40 kHz. The lamp was filled with hydrogen (>99.995%) at 45 kPa. The intensity level of the emission beam was adjusted so that 800 fluorescence photons or less were observed per second. The fluorescence measurements were performed at right angle observation of the center of a centrally illuminated cuvette (1 × 1 × 4 cm) in L- or T-format. Front-face illumination was performed using triangular cuvettes oriented 45° relative to the incident beam at 25 °C. Where applicable, solutions were purged with nitrogen for 10 min in the cuvette and then stoppered. Solutions of the stereoregular PMMA were measured 22 h after the mixing of solutions of i-PMMA and s-PMMA.

Results and Discussion

Fluorescence Quantum Yield of Carbazole in CEMA and in a-PMMA-C. From corrected emission spectra of the carbazole fluorophore in the CEMA and copolymer a-PMMA-C in several solvents, we have determined the relative fluorescence quantum yield Q_D (Table 2). The value of the fluorescence quantum yield of the carbazole fluorophore in the side chains of the polymer is higher than for low molecular weight monomer CEMA. A decrease in the mobility of the fluoro-

Table 3. Efficiency of Nonradiative Energy Transfer (E) in Tactic Polymer System i-PMMA-C/s-PMMA-A in Dimethylformamide and Dioxane (τ_C, τ_{CA} = Lifetimes of Carbazole Fluorophore in the Absence and Presence of the Acceptor; C_{POL} = Overall Polymer Concentration; C_C, C_A = Carbazole and Anthracene Concentrations)

C_{POL} (g L^{-1})	$10^4 C_C$ (mol L^{-1})	$10^4 C_A$ (mol L^{-1})	τ_{CA} (ns)	τ_C (ns)	E
		Dimethylformamide			
2.5	1.30	3.0	10.8	13.2	0.18
5.0	2.61	6.0	10.7	13.2	0.19
10.0	5.22	12.0	11.0	13.7	0.20
		Dioxane			
2.5	1.30	3.0	11.9	13.2	0.10
5.0	2.61	6.0	12.2	13.6	0.10
10.0	5.22	12.0	12.6	13.8	0.09

phore attached to the polymer chain results in a decrease of the rate of radiationless transitions.

Efficiency of Nonradiative Energy Transfer. The characteristic distance R_0 according to Förster's theory (eq 2) expected in the absence of fluorophore difussion is given in Table 2. The characteristic concentration of carbazole (anthracene) $C_{0.5}$ (mol/L) corresponding to $E = 0.5$ may be obtained from the experimental data defining a characteristic distance r_o (nm) for NET given by[31] $r_o = 0.735/(C_{0.5})^{1/3}$ (nm). The characteristic distance r_o depends on the content of the fluorophores in the labeled atactic PMMA and on the translational diffusion coefficient of the polymer molecules. It is quite obvious that translational diffusion of the polymer coils during the excited state lifetime of the carbazole fluorophore in the polymer solution will play an important role.

For low molecular weight compounds, the distance r_o is usually longer than R_o. The diffusion of the donor fluorophores toward the acceptor during the excited state lifetime of the donor is probably the cause of this difference.[33]

An increase in the lifetime of the excited state of the carbazole fluorophore embedded in the atactic copolymer (a-PMMA-C) in the mixture with unlabeled atactic PMMA was observed with increasing concentration of polymer in dioxane and DMF (for a-PMMA-C and unlabeled PMMA in DMF at concentration 9.25 g/L and 185.00 g/L the lifetimes are 13.50 and 14.50 ns, respectively). The increase in the concentration of a polymer mixture in solution causes an increase in viscosity. This results in a decreased mobility of the fluorophore and consequently causes a decrease in the rate of radiationless transitions.

With increasing concentration of fluorophores in the system a-PMMA-C/a-PMMA-A, the decrease in the lifetime of the excited state of the donor in the presence of the acceptor (τ_{CA}) becomes more pronounced. Assuming a double exponential decay, the contribution of the short lifetime component should increase with an increasing concentration of fluorophores. The efficiency of NET was characterized by the lifetimes obtained from the best single exponential fit. To estimate the dependence of the lifetimes of the carbazole fluorophore in the absence of the acceptor on the polymer concentration, unlabeled polymer was added to the system.

As previously shown by different experimental methods, stereocomplex formation between isotactic and syndiotactic polymers occurs at a 1:2 ratio of i-PMMA/s-PMMA.[1,2] Therefore, the efficiency of NET was determined at this ratio for the mixture of labeled isotactic (i-PMMA-C) and syndiotactic (s-PMMA-A) polymers (Table 3) and the corresponding labeled atactic polymers a-PMMA-C and a-PMMA-A (Table 4). Fluorescence measurements were carried out for solutions of low optical density at right angle observation (excitation wavelength 307 nm) and for high optical density solutions from front-face illumination (excitation wavelength 292 nm). Emission of the carbazole fluorophore was monitored at a wavelength of 360 nm. The same value of E was found for excitation at 292 or 307 nm. The lifetimes of the carbazole fluorophore under a nitrogen atmosphere were in all cases longer than those under air. Oxygen quenching of carbazole fluorescence in the absence of the acceptor is proportional to oxygen quenching of carbazole in the presence of the anthracene fluorophore, so that the efficiency of NET is the same in aerated and deaerated solutions.

Table 4. Efficiency of Nonradiative Energy Transfer (E) in Atactic Polymer System a-PMMA-C/a-PMMA-A in Dimethylformamide and Dioxane (Symbols Are the Same as in Table 3)

C_{POL} (g L^{-1})	$10^4 C_C$ (mol L^{-1})	$10^4 C_A$ (mol L^{-1})	τ_{CA} (ns)	τ_C (ns)	E
		Dimethylformamide			
4.071	1.30	3.0	12.1	12.6	0.04
8.143	2.61	6.0	11.9	12.5	0.05
16.286	5.20	12.0	11.2	13.0	0.14
		Dioxane			
4.071	1.30	3.0	12.8	13.2	0.03
8.143	2.61	6.0	12.7	13.4	0.05
16.286	5.20	12.0	12.0	13.2	0.09

Nonradiative energy transfer is more efficient for the polymer mixture consisting of labeled stereoregular polymers (Table 3) than in the mixture of atactic polymers (Table 4). It should be noted that in both copolymers, the donor fluorophore content is low, so that their domains do not overlap and migration of the excitation energy does not take place. As expected for a mixture of noncomplexing atactic polymers, the efficiency of NET increases with increasing polymer (fluorophore) concentration. On the other hand in complexing solvents (DMF and dioxane) the efficiency of NET for tactic PMMA is nearly independent of the polymer concentration. The formation of the stereocomplex at different concentrations of tactic PMMA fixes a distance between the donor and acceptor fluorophores within the complex and makes E insensitive to overall polymer concentration. This is illustrated in Figure 3.

Another indication of stereocomplex formation is a change in the I_C/I_A ratio with incubation time. The decay I_C/I_A with time reflects the stereocomplex formation (Figure 4). This demonstrates that fluorescent labels of i-PMMA and s-PMMA approach each other as the complex is formed. Also, the figure shows qualitatively that the complex is formed faster in DMF than in dioxane, as found by another method.[1] Unfortunately, the initial phase of stereocomplex formation is too fast to be followed by our experimental method. For the same reason the time dependence of the efficiency of NET could not be evaluated using the average lifetime of the excited state measurements. The initial value of I_C/I_A before the stereocomplex is formed can be obtained using atactic PMMA with the same fluorophore content in labeled polymers and comparable molecular weights and overall concentration of polymers. It can be estimated that ~65% of the change in this ratio took place before the first reading could be taken in the solution containing the mixture of isotactic and syndiotactic PMMA. For chloroform, the I_C/I_A ratio is constant since no stereocomplex is formed in that medium.

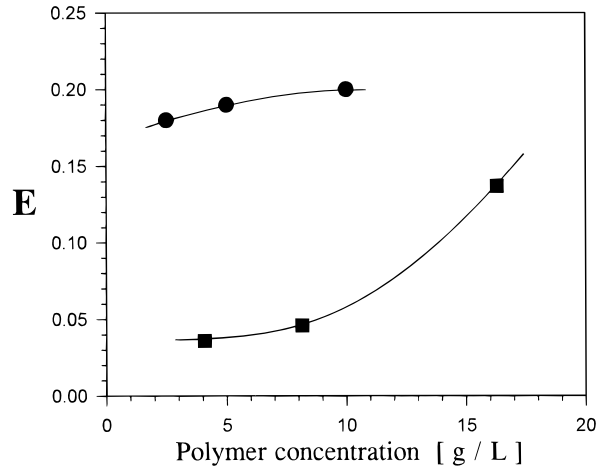

Figure 3. Efficiency of nonradiative energy transfer (E) as a function of polymer concentration for atactic a-PMMA-C/a-PMMA-A (■) and tactic i-PMMA-C/s-PMMA-A (●) polymer systems in dimethylformamide.

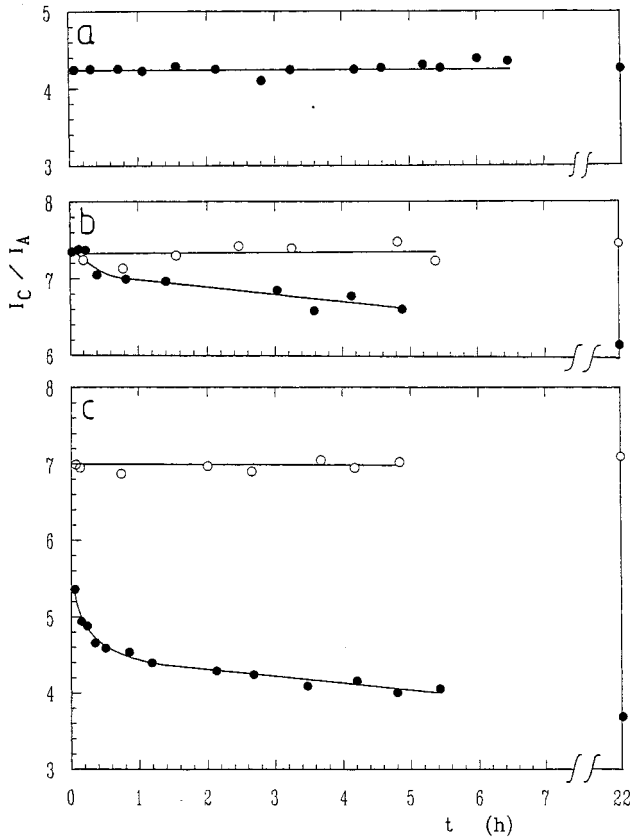

Figure 4. Time dependence of I_C/I_A for labeled stereoregular (●) and atactic (○) PMMA in chloroform (a) ($C_{POL} = 22$ g L^{-1}; $C_C = C_A = 5.0 \times 10^{-4}$ M), dioxane (b), and dimethylformamide (c) (in both solvents: $C_{POL} = 8.80$ g L^{-1}; $C_C = C_A = 2.0 \times 10^{-4}$ M).

Micro-Brownian Relaxation of Poly(methyl methacrylate)s in Solution. Generally, it is expected that stereocomplex formation between i-PMMA and s-PMMA will influence the mobility of a fluorophore either situated in the side chain of the polymer molecule or embedded in the polymer backbone.[34] Comparison of these data with data obtained for mixtures of atactic poly(methyl methacrylate)s might supply additional information on stereocomplex formation.

Fluorescence depolarization has been used to study segmental relaxations of macromolecules in solution by several researchers.[35,36] Most studies on micro-Brownian rotational motions have employed the less informative steady-state emission polarization.[36]

In the analysis of time-resolved decays of anisotropy, one generally fits the observed values to a sum of exponential decays (eq 5). To describe the time-resolved decays of anisotropy, a biexponential fit is in most cases satisfactory.

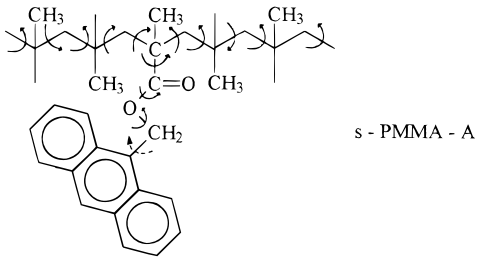

Figure 5. Relative backbone geometries. Full arrows represent motions resulting in depolarization of emitted radiation. Broken arrows represent motion that do not result in fluorescence depolarization.

Table 5. Rotational Correlation Times of the Carbazole and Anthracene Fluorophore (Φ, Single Exponential Fit) for Atactic Polymer Systems in Dimethylformamide and Dioxane ($C_{POL} = 8.143$ g L^{-1}; $C_C = 2.61 \times 10^{-4}$ M; $C_A = 6.00 \times 10^{-4}$ M)

		Φ (ns)	
polymer system	fluorophore	DMF	dioxane
a-PMMA-C/a-PMMA	carbazole	2.3	1.7
a-PMMA/a-PMMA-A	anthracene	1.8	2.3

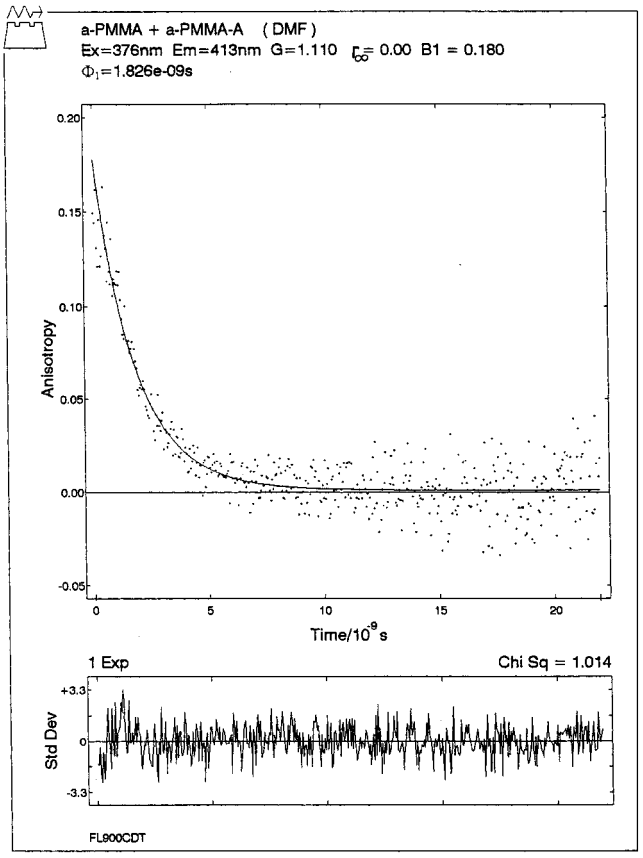

Figure 6. Time dependence of the emission anisotropy (r) for a-PMMA/a-PMMA-A in dimethylformamide ($C_{POL} = 8.143$ g L^{-1}, $C_A = 6.00 \times 10^{-4}$ M). Φ is the rotational correlation time of the anthracene fluorophore, r_∞ is the limiting anisotropy, for G factor see eq 8, and B is the pre-exponential factor (see eq 5).

Table 6. Rotational Correlation Times of the Carbazole and Anthracene Fluorophore (Φ_1, Φ_2 = Double Exponential Fit) for Tactic Polymer Systems in Different Solvents (i/s = 1/2; C_{POL} = 5.00 g L^{-1}; $C_C = 2.61 \times 10^{-4}$ M; $C_A = 6.00 \times 10^{-4}$ M)

fluorophore	Φ_1 (ns)	Φ_2 (ns)	rel B_2 (%)
	Dimethylformamide		
carbazole	25.5	1.4	14
anthracene	11.9	2.0	32
	Dioxane		
carbazole	19.1	1.2	29
anthracene	7.3	1.6	50
	Chloroform		
carbazole		1.3	
anthracene		1.1	

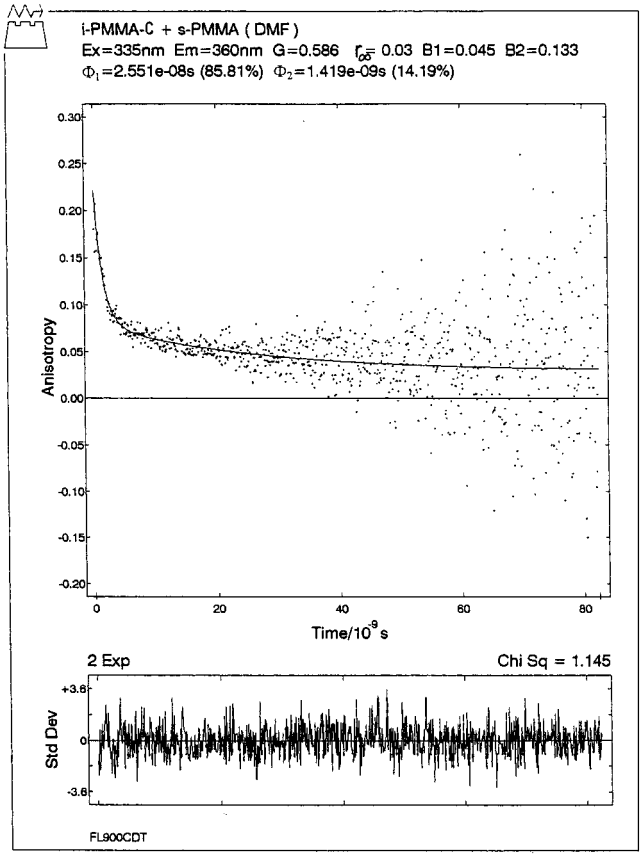

Figure 7. Time dependence of the emission anisotropy (r) for i-PMMA-C/s-PMMA in dimethylformamide (i/s = 1/2, C_{POL} = 5.00 g L^{-1}, $C_C = 2.61 \times 10^{-4}$ M). Φ_1 and Φ_2 are the rotational correlation times of the carbazole fluorophore. For r_∞, G, and B, see Figure 6.

Consider a fluorophore bound to a synthetic polymer molecule with the fluorophore undergoing motions that reflect the position of the fluorophore in the polymer molecule. Figure 5 shows the orientation of the label with respect to the chain backbone for a copolymer of methyl methacrylate with the (9-anthryl)methyl methacrylate (s-PMMA-A). In s-PMMA-A, the transition dipole corresponding to absorption and emission is not oriented parallel to the bond of attachment to the chain. Therefore, a motion independent of the chain should produce depolarization in addition to that caused by the mobility of the polymer segments.

It should be noted that the rotational diffusion of the macromolecules as a whole is much slower than local conformational transitions,[37,38] and the depolarization of fluorescence may be interpreted in terms of the conformational mobility of the polymer chain segments

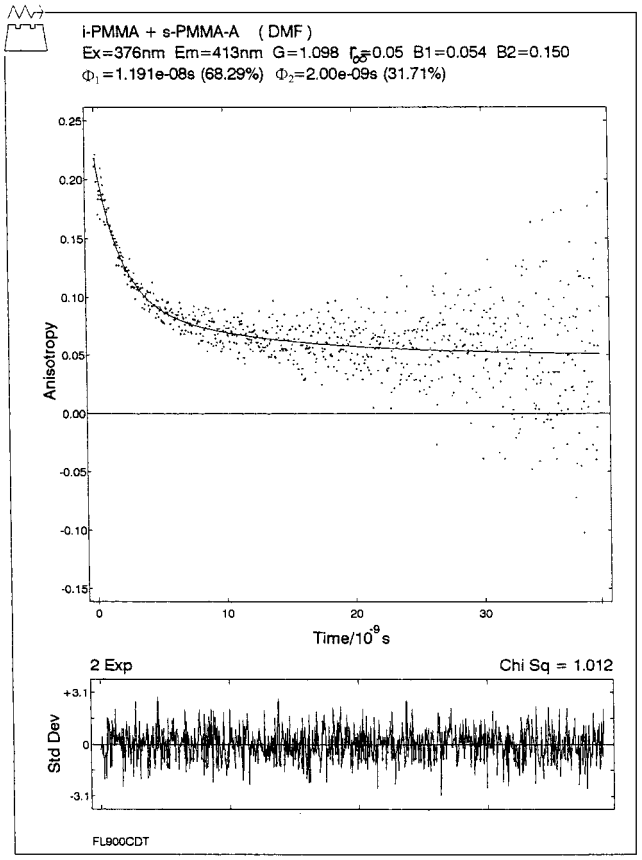

Figure 8. Time dependence of the emission anisotropy (r) for i-PMMA/s-PMMA-A in dimethylformamide (i/s = 1/2, C_{POL} = 5.0 g L^{-1}, $C_A = 2.61 \times 10^{-4}$ M). For Φ_1, Φ_2, r_∞, G, and B, see Figures 6 and 7.

and the mobility of the side group with attached fluorescence label.

The intramolecular motion in which a fluorophore participates may then be expressed by[39]

$$\frac{1}{\Phi_i} = \frac{1}{\Phi_s} + \frac{1}{\Phi_b} \tag{9}$$

where Φ_s and Φ_b are rotational correlation times of the side chain of the polymer and polymer backbone segment, respectively. The time-resolved decays of anisotropy for the mixture of noncomplexing atactic polymers (Table 5, Figure 6) in different solvents can be assumed to be monoexponential. Low values of the rotational correlation times evaluated for the anthracene fluorophore in the mixture of noncomplexing PMMA can be assigned to the fast relaxation motion of the side chain with attached anthracene fluorophore and segmental relaxation of the polymer backbone. For comparison, the rotational correlation time of low molecular weight 9,10-dimethylanthracene in chloroform is 0.4 ns.

A dramatic change in the time-resolved decay of anisotropy was observed for mixtures of labeled tactic PMMA (Table 6, Figures 7 and 8). The limiting anisotropy (r_∞) for both fluorophores is larger than zero. Values larger than zero demonstrate steric hindrance for rotation caused by stereocomplex formation. The time-resolved decay curves are double-exponential for solvents that support formation of the stereocomplex (DMF and dioxane) and monoexponential for noncomplexing solvent (chloroform). The long rotational correlation time (Φ_1) demonstrates formation of the stereocomplex. In the strongly complexing solvent DMF,

the rotational correlation times are longer than in the weakly complexing solvent (dioxane) and the fractional contribution (rel B_2) of motion with shorter correlation time is smaller in DMF than in dioxane. The long time component of the relaxation process was found for both fluorophores, i.e., in the mixtures of polymers i-PMMA-C/s-PMMA and i-PMMA/s-PMMA-A. In the noncomplexing solvent, chloroform, no long time component has been found. The formation of a stereocomplex brings about a decrease in the mobility of the polymer segments and side chains of polymers producing the increase in the rotational relaxation time.

The polymer with a label bound to the end of the side chain containing the ester group, s-PMMA-A, yields a correlation time in chloroform of 1.1 ns. Similar rotational relaxation times as for the anthracene fluorophore in the same solvent were observed for the carbazole fluorophore in the side chains of tactic and atactic polymers. The rotational correlation time of intramolecular motion of associated polymer chains in the stereocomplex containing i-PMMA-C was longer than that containing s-PMMA-A. If we suppose that the stereocomplex consists of a double-stranded helix[40] in which an i-chain is surrounded by a s-chain, the fact that the anthracene label is more mobile than the carbazole label may be due to the attachment of the anthracene label on the outer s-chain of the stereocomplex. By comparison of values of intramolecular rotational correlation times of polymer segments in stereocomplexes (Table 6), those formed in dimethylformamide are more compact than those formed in dioxane.

Conclusions

NET has been employed to investigate the formation of a stereocomplex between isotactic and syndiotactic PMMA. The efficiency of NET between the donor and acceptor fluorophores embedded in the tactic PMMA depends on the solvent. In the strongly complexing solvent (DMF) the efficiency of NET is larger than that in weakly complexing solvent (dioxane) and is nearly independent of the polymer concentration. In mixtures of the labeled atactic PMMA, the efficiency of NET between fluorophores does not depend on solvent but depends on polymer concentration in solution.

The time dependence of the ratio of fluorescence intensity of the donor (carbazole) to the fluorescence intensity of the acceptor (anthracene) clearly demonstrates formation of a stereocomplex between labeled isotactic and syndiotactic PMMA chains.

The increase in the rotational correlation times of the carbazole and anthracene fluorophores embedded in tactic polymers reflects the formation of a stereocomplex in dimethylformamide and dioxane. The larger decrease in the mobility of the carbazole fluorophore attached to isotactic polymers allows us to speculate that an isotactic chain is surrounded by a syndiotactic chain in the stereocomplex.

Acknowledgment. We are grateful to Professor Herbert Morawetz for stimulating discussions and his help in preparation of this manuscript. We also thank the Academy of Sciences of the Czech Republic for their support of this work by grant 12/96/K.

References and Notes

(1) Spěváček, J.; Schneider, B. *Adv. Colloid Interface Sci.* **1987**, *27*, 81.
(2) Pokorná, V.; Mikeš, F.; Pecka, J.; Vyprachtický, D. *Macromolecules* **1993**, *26*, 2139.
(3) Förster, T. *Ann. Phys.* (*Leipzig*) **1948**, *2*, 55.
(4) Förster, T. *Discuss. Faraday Soc.* **1959**, *27*, 7.
(5) Förster, T. *Compr. Biochem.* **1967**, *22*, 61.
(6) Steinberg, I. Z. *Annu. Rev. Biochem.* **1971**, *40*, 83.
(7) Amrani, F.; Hung J. M.; Morawetz, H. *Macromolecules* **1980**, *13*, 649.
(8) Mikeš, F.; Morawetz, H.; Dennis, K. S. *Macromolecules* **1980**, *13*, 969; **1984**, *17*, 60.
(9) Morawetz, H. *Ann. N. Y. Acad. Sci.* **1981**, *366*, 404.
(10) Katchalski-Katzir, E.; Steinberg, I. Z. *Ann. N. Y. Acad. Sci.* **1981**, *366*, 44.
(11) Liu, G.; Guillet, J. E.; Al-Takrity, E. T. B.; Jenkins, A. D.; Walton, D. R. M. *Macromolecules* **1990**, *23*, 1393; **1991**, *24*, 68.
(12) Winnik, F. M. *Polymer* **1990**, *31*, 2125.
(13) Horský, J.; Morawetz, H. *Makromol. Chem.* **1988**, *189*, 2475.
(14) Winnik, F. M. *Macromolecules* **1989**, *22*, 734.
(15) Ringsdorf, H.; Simon, J.; Winnik, F. M. *Macromolecules* **1992**, *25*, 5353.
(16) Pekcan, Ö.; Egan, S. S.; Winnik, M. A.; Croucher, M. D. *Macromolecules* **1990**, *23*, 2110.
(17) Winnik, M. A.; Wang, Y.; Holey, F. *J. Coat. Technol.* **1992**, *64* (811), 51.
(18) Morawetz, H. *Science* **1988**, *240*, 172.
(19) Morawetz, H. *Collect. Czech. Chem. Commun.* **1993**, *58*, 2266.
(20) Simionescu, C. I.; Grigoras, M.; David, G. *Makromol. Chem.* **1989**, *190*, 1537.
(21) Otsuki, H.; Okano, J.; Takeda, T. *J. Soc. Chem. Ind. Jpn.* **1946**, *49*, 169.
(22) Hargreaves, J. S.; Webber, S. E. *Macromolecules* **1984**, *17*, 235.
(23) Hatada, K.; Ute, K.; Tanaka, K.; Kitayama, T.; Okamoto, Y. *Polym. J.* **1985**, *17*, 977.
(24) Abe, H.; Imai, K.; Matsumoto, M. *J. Polym. Sci., Part C* **1968**, *23*, 469.
(25) Bovey, F. A.; Tiers, G. V. *J. Polym. Sci.* **1960**, *44*, 173.
(26) Lakowicz, J. R. *Principles of Fluorescence Spectroscopy*; Plenum Press, New York 1983; pp 40, 161, and 309.
(27) Lippert, E.; Nagelle, W.; Seibold-Blakenstein, I.; Staiger, U.; Voss, W. *Z. Anal. Chem.* **1959**, *17*, 1.
(28) Argauer, R. J.; White, C. E. *Anal. Chem.* **1964**, *36*, 368.
(29) Melhuish, W. H. *J. Phys. Chem.* **1960**, *64*, 762.
(30) Parker, C. A. *Photoluminescence of Solutions*; Elsevier Publishing Co.: Amsterdam, London, New York, 1968.
(31) Berlman, I. B. *Handbook of Fluorescence Spectra of Aromatic Molecules*; Academic Press: New York, 1971; p 205.
(32) Maximov, M. Z.; Rozman, I. M. *Opt. Spectrosc.* **1962**, *12*, 337.
(33) Elkana, Y.; Feitelson, J.; Katchalski, E. *J. Chem. Phys.* **1968**, *48*, 2399.
(34) Pokorná, V.; Vyprachtický, D.; Pecka, J.; Mikeš, F. Manuscript in preparation.
(35) Valeur, B.; Monnerie, L. *J. Polym. Sci., Phys. Ed.* **1976**, *14*, 11.
(36) Nekrasova, T. N.; Anufrieva, E. V.; Krakovyak, M. G.; Lushik, V. B.; Korshun, A. M. *Vysokomol. Soyed.* **1983**, *A25*, 133.
(37) Anufrieva, E. V.; Volkenstein, M. V.; Gotlib, Yu. Ya.; Krakovyak, M. G.; Skorochodov, S. S.; Sheveleva, T. V. *Dokl. Akad. Nauk. SSSR* **1970**, *194*, 1108.
(38) Biddle, D.; Nordström, N. *Ark. Kemi* **1970**, *32*, 359.
(39) Anufrieva, E. V.; Gotlib, Yu. Ya. *Adv. Polym. Sci.* **1981**, *40*, 1.
(40) Bosscher, F.; Brinke, G. T.; Challa, G. *Macromolecules* **1982**, *15*, 1442.

MA970934G